

Effect of growth interruption in 1.55 μm InAs/InAlGaAs quantum dots on InP grown by molecular beam epitaxy

Daehwan Jung, Daniel J. Ironside, Seth R. Bank, Arthur C. Gossard, and John E. Bowers

Citation: *Journal of Applied Physics* **123**, 205302 (2018); doi: 10.1063/1.5031772

View online: <https://doi.org/10.1063/1.5031772>

View Table of Contents: <http://aip.scitation.org/toc/jap/123/20>

Published by the *American Institute of Physics*

PHYSICS TODAY

WHITEPAPERS

MANAGER'S GUIDE

Accelerate R&D with
Multiphysics Simulation

READ NOW

PRESENTED BY

 **COMSOL**

Effect of growth interruption in 1.55 μm InAs/InAlGaAs quantum dots on InP grown by molecular beam epitaxy

Daehwan Jung,¹ Daniel J. Ironside,² Seth R. Bank,² Arthur C. Gossard,^{1,3} and John E. Bowers^{1,3}

¹*Institute for Energy Efficiency, University of California Santa Barbara, Santa Barbara, California 93106, USA*

²*Electrical and Computer Engineering, University of Texas Austin, Austin, Texas 78705, USA*

³*Department of Electrical and Computer Engineering, University of California Santa Barbara, Santa Barbara, California 93106, USA*

(Received 30 March 2018; accepted 5 May 2018; published online 23 May 2018)

We report the effect of growth interruptions on the structural and optical properties of InAs/InAlGaAs/InP quantum dots using molecular beam epitaxy. We find that the surface quantum dots experience an unintended ripening process during the sample cooling stage, which reshapes the uncapped InAs nanostructures. To prevent this, we performed a partial capping experiment to effectively inhibit structural reconfiguration of surface InAs nanostructures during the cooling stage, revealing that InAs nanostructures first form quantum dashes and then transform into quantum dots via a ripening process. Our result suggests that the appearance of buried InAs/InAlGaAs nanostructures can be easily misunderstood by surface analysis. *Published by AIP Publishing.* <https://doi.org/10.1063/1.5031772>

I. INTRODUCTION

Self-assembled InAs quantum dots (QDs) are a promising light source for 1.55 μm telecommunication wavelength lasers with low threshold current densities, low thermal dependence, and large material modal gain.^{1–3} The InAs/GaAs QD lasers emitting at 1.3 μm wavelength have been extensively studied, and now, they outperform the conventional quantum well (QW) counterparts in many aspects. However, it is known that high quality InAs/InP QDs are more difficult to grow than InAs/GaAs QDs largely due to the reduced lattice mismatch between InAs and InP.^{4,5} Moreover, InAs nanostructures on InP substrates tend to form quantum dashes (QDashes) rather than QDs because of the strong surface diffusion anisotropy of In adatoms.^{6,7} To fully exploit the advantages of zero-dimensional quantum structures, various approaches have been investigated to realize round-shaped InAs QDs on InP substrates.

One approach is to use high-index InP substrates such as (113) orientation.⁸ The reduced indium surface diffusion anisotropy on the (113) orientation enabled high performance InAs/InGaAsP QD lasers on InP substrates with a QD density of $1.1 \times 10^{11} \text{ cm}^{-2}$.⁹ On a more conventional (001) orientation, systematic studies have been conducted to control the morphology of InAs QDs using molecular beam epitaxy (MBE). Gilfert *et al.* found that using As_2 molecules over As_4 for their InAs/InAlGaAs QDs helps achieve more round-shaped QDs.¹⁰ Also, Kim *et al.* reported that inserting a thin GaAs pre-layer prior to InAs deposition controls the structural properties of InAs QDs.¹¹ Similarly, it was reported that the growth condition of an InAlGaAs buffer layer can significantly affect the QD morphology and densities.^{12,13} On the contrary, Stintz *et al.* argued that the InAs nanostructure is largely determined by the number of InAs monolayers (MLs), independent from other factors such as buffer layer growth condition.¹⁴

Another important growth parameter for InAs QD morphology is growth interruption (GI), which often allows QDs to reorganize through a ripening process before they are capped by a subsequent layer. Although extensive studies about the GI effect have been reported for the case of InAs/GaAs QDs, InAs/InP (001) QDs have been relatively unexplored. Poole *et al.* used planar view transmission electron microscopy (TEM) to show that increasing GI time from 10 s to 20 s transformed the InAs nanostructure morphology from QDashes to QDs when they were grown on InP buffers.¹⁵ Wang *et al.* reported that a 10 s GI caused red-shift of photoluminescence (PL) peaks and increased the InAs QD size using metal-organic chemical vapor deposition.¹⁶ Although high performance InAs/InAlGaAs QD lasers grown on InP have been demonstrated by several groups using molecular beam epitaxy,^{17–19} no studies have been reported about the effect of GI in the InAs/InAlGaAs QD structural and optical properties.

In this work, we show that formation of InAs/InAlGaAs QDs is heavily dependent on the duration of GI time. PL peaks showed significant red-shifts from the InAs QDs when the GI time was increased, indicating a structural transformation of the buried QDs. However, the atomic force microscopy (AFM) measurements on the uncapped surface QDs with GI revealed no change in the QD morphology. It was thought that the uncapped QDs experienced an unintended ripening process during the cooling stage due to the remaining heat in the substrate heater. We partially covered the surface InAs QDs by depositing a 3 nm $\text{In}_{0.50}\text{Al}_{0.35}\text{Ga}_{0.15}\text{As}$ layer after the GI to avoid the unintended ripening process during sample cooling. The partial capping effectively inhibited the surface QD reorganization and preserved the as-grown InAs nanostructures while cooling down to room temperature for sample removal. The AFM images indicate that a sufficient GI time is required to form round-shaped InAs QDs over QDashes. Cross-sectional TEM (X-TEM) confirmed the

effect of GI in the buried InAs/InAlGaAs nanostructures by showing dissimilar InAs nanostructure morphologies along $[110]$ and $[1\bar{1}0]$ orientations.

II. EXPERIMENTAL DETAILS

Figure 1(a) shows an InAs/InAlGaAs QD sample structure for PL and AFM measurements. All samples were grown by solid source molecular beam epitaxy. A semi-insulating InP (001) substrate was desorbed at 510°C under As_2 overpressure to completely remove oxide. A 250 nm $\text{In}_{0.53}\text{Al}_{0.24}\text{Ga}_{0.23}\text{As}$ (InAlGaAs) buffer was grown lattice-matched (LM) to InP at 500°C , as measured by optical pyrometer, followed by a growth interruption to decrease the substrate temperature to 485°C for InAs QD growth. Before InAs QD deposition, ~ 2 monolayers (MLs) of $\text{Al}_{0.5}\text{Ga}_{0.5}\text{As}$ (~ 0.6 nm) was grown to induce blue-shift in the QD emission wavelength and to slow down the indium adatom mobility.^{20,21} 7 MLs of InAs were deposited for PL measurement at a growth rate of 0.42 ML/s. The V/III ratio was kept at ~ 17 , and As_2 molecules were used to induce QDs over QDashes.¹⁰ Various GI times from 0 to 60 s were applied before the QDs were covered by a 3 nm thick $\text{In}_{0.50}\text{Al}_{0.35}\text{Ga}_{0.15}\text{As}$ partial capping layer at 485°C . Then, the substrate temperature was raised back to 500°C under As_2 overpressure, followed by a 250 nm thick LM InAlGaAs spacing layer. The surface InAs QDs for AFM measurement was grown in the same growth condition as the buried PL QDs. The sample was immediately quenched to room temperature under As_2 overpressure for AFM measurement. For PL experiments, the samples were optically pumped using a 532 nm laser (photon energy significantly greater than the bandgap of InAlGaAs matrix and InP substrate), and PL emission was collected by a spectrometer with a liquid nitrogen-cooled InSb detector. A Veeco Dimension 3100 AFM and Bruker FMV-A tips were used to investigate the morphology of the uncapped and partially capped surface QDs. Transmission electron microscopy was performed with a FEI Tecnai G2 200 keV TEM after mechanically grinding and Ar ion-milling specimens.

III. RESULTS

A. Without growth interruption

Figures 1(b) and 1(c) show the QD morphology and room-temperature (RT) PL spectra from the reference

sample (GI time = 0 s, no partial capping for surface QDs). The AFM image reveals round-shaped InAs QDs with a QD density of $6.5 \times 10^{10} \text{ cm}^{-2}$. The average dot diameter is ~ 25 nm and height is ~ 7 nm. The majority of the QDs grew in a round shape, and only some of them take elongated shapes with smaller heights. The reference sample has a PL peak wavelength at $1.58 \mu\text{m}$ at RT, as shown in Fig. 1(c). The measured full-width at half-maximum (FWHM) is 70.3 meV, which is comparable to other previously reported values.^{11,22,23}

B. Growth interruptions

To investigate the GI effect in the optical and structural property of the InAs/InAlGaAs QDs, we applied various GI times (5, 10, 20, and 60 s) before capping the InAs QDs by a subsequent 3 nm $\text{In}_{0.50}\text{Al}_{0.35}\text{Ga}_{0.15}\text{As}$ partial capping layer. For the surface QDs, an equal GI time was applied before they were cooled down to RT for sample removal, but “no partial capping” was applied to these samples. The AFM images of Figs. 2(a) and 2(b) show that the InAs QDs with 5 s and 60 s GI look almost identical to the reference sample shown in Fig. 1(b). The dot density is $6.5 \times 10^{10} \text{ cm}^{-2}$ with an average height of ~ 7.5 nm. However, Fig. 2(c) shows clear PL red-shifts from $1.63 \mu\text{m}$ to $1.78 \mu\text{m}$ as the GI time increases from 5 s to 60 s.

The red-shift of the PL peaks indicates the evolution of the buried InAs nanostructure morphology during the GI, which is contrary to the observation of the surface InAs QDs from our AFM measurements. The red-shift was caused by the reduced quantum confinement effect in the QDs, which occurs in both lateral and vertical directions. However, it should be noted that the height of our InAs/InAlGaAs QDs is about 3 times smaller than the lateral dimensions. Therefore, the fact that the PL showed red-shifts with increasing GI times strongly suggests the formation of taller InAs nanostructures. The increasing FWHM also indicates that partial capping by the 3 nm $\text{In}_{0.50}\text{Al}_{0.35}\text{Ga}_{0.15}\text{As}$ layer for the buried InAs QDs does not control the height dispersion of the InAs nanostructures, which is contradictory to the case of InAs/InGaAsP QD system.²⁴

We speculated that inefficient sample removal resulted in unintentional ripening of the uncapped surface InAs nanostructures and allowed for QD structure modification. Krzyzewski *et al.* showed that a significant change in InAs/GaAs QD morphology and density can occur during the

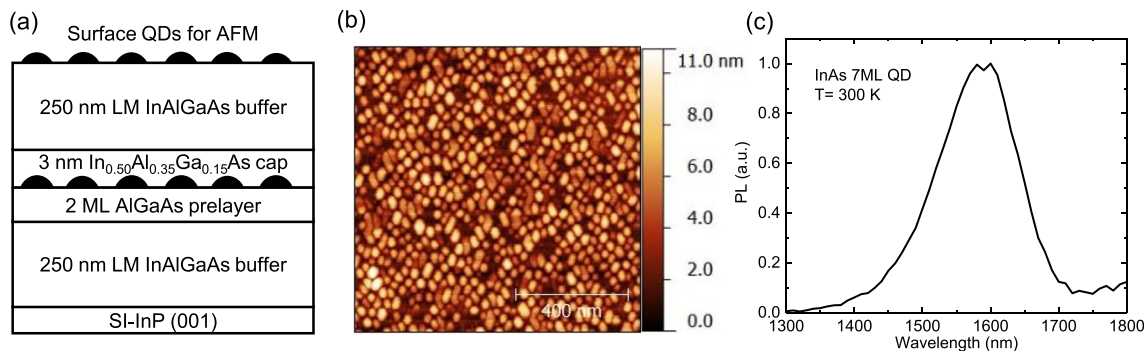


FIG. 1. (a) A schematic of InAs/InAlGaAs QD structure for PL and AFM measurements. (b) $1 \times 1 \mu\text{m}^2$ AFM image from the reference sample without GI time and partial capping. (c) Room-temperature PL spectrum from the reference QD sample.

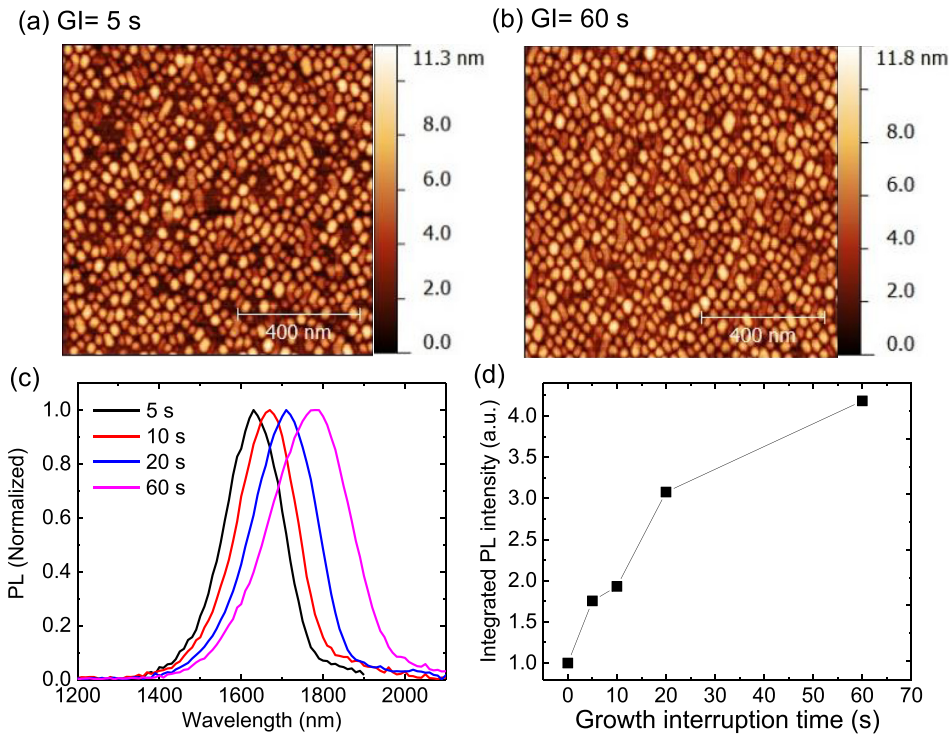


FIG. 2. Effect of ripening time in InAs/InAlGaAs QDs. The surface QDs are *not partially capped*. (a) $1 \times 1 \mu\text{m}^2$ AFM image from sample with GI = 5 s. (b) $1 \times 1 \mu\text{m}^2$ AFM image from sample with GI = 60 s. (c) PL spectra from samples with various GI times. (d) Integrated RT PL intensity as a function of GI time.

cooling stage, and this can misrepresent the structural information about the capped QDs underneath.²⁵ They showed that the average InAs/GaAs QD density and volume can vary by a factor of 2.5 depending on the rapidness of the quench method. It should be noted that a much higher InAs growth rate (~ 0.4 ML/s) is typically used for InAs/InP QDs compared with that for InAs/GaAs QD system (~ 0.1 ML/s).^{10,26,27} This suggests that the growth of InAs nanostructure on InP is more kinetically limited than on GaAs by MBE and that ripening process during growth interruption can

influence the morphology of InAs/InP QDs more significantly than that of InAs/GaAs QDs.

C. Growth interruptions with partial capping

In order to prevent the unintended ripening of the surface QDs during sample quenching, we have conducted a partial capping experiment. Various GI times were applied for the surface QDs and a 3 nm thick $\text{In}_{0.50}\text{Al}_{0.35}\text{Ga}_{0.15}\text{As}$ partial capping layer was deposited before cooling down for

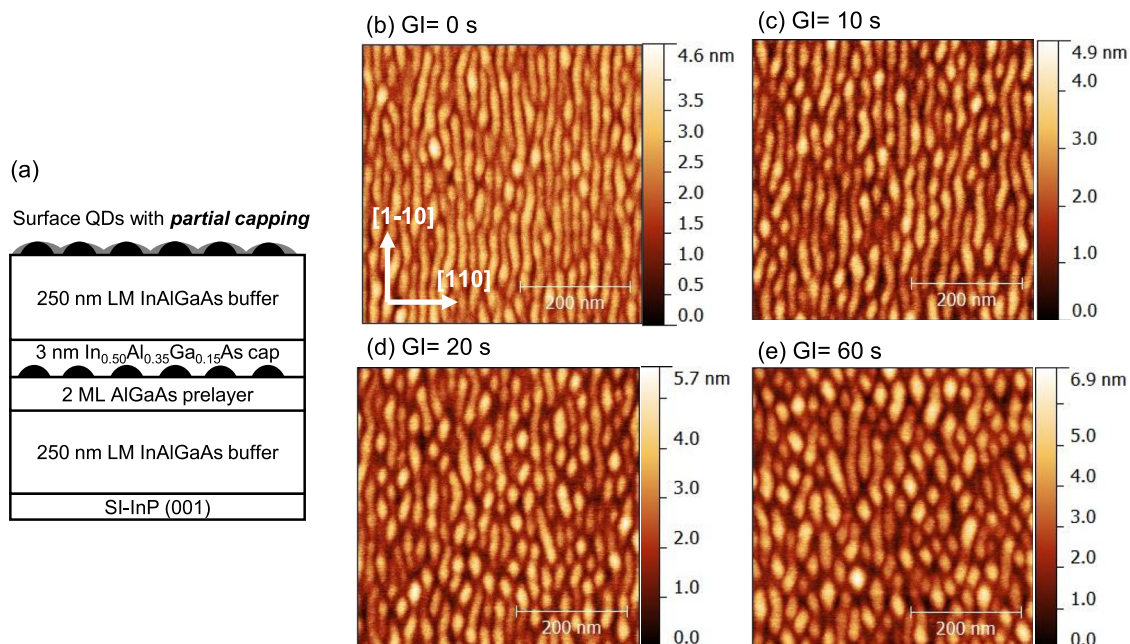


FIG. 3. (a) A schematic of InAs/InAlGaAs QD structure with surface QD partial capping after various GI times. $500 \times 500 \text{ nm}^2$ AFM images from partially capped InAs QD samples with various GI times of (b) GI = 0 s, (c) GI = 10 s, (d) GI = 20 s, and (e) GI = 60 s.

sample removal as shown in Fig. 3(a). The use of the partial capping effectively prevented the reorganization of the surface InAs QDs during quenching. Figures 3(b)–3(e) show the evolution of the InAs nanostructure morphology as the GI time increases from 0 s to 60 s. First, when the GI time is 0 s, the InAs nanostructure morphology takes elongated QDashes, which is far different from the reference sample (GI = 0 s) but without the partial capping layer [Fig. 1(b)]. Note that all the other growth conditions were kept identical. The elongation orientation is in $[1\bar{1}0]$ direction due to the faster In adatom surface diffusion on an As-stabilized surface.^{10,28} The density of the InAs QDashes is $5.1 \times 10^{10} \text{ cm}^{-2}$. As we increase the GI time from 0 s to 10 s, it was observed that the InAs nanostructure reorganizes the structure into more round-shapes with increased heights. Finally, when the GI time was increased to 60 s, the InAs nanostructure showed round-shaped QDs with minimal elongation into $[1\bar{1}0]$ direction. The QD density from the 60 s GI sample is $6.1 \times 10^{10} \text{ cm}^{-2}$, which is similar to the reference sample (GI = 0 s) with no partial capping.

The surface QDs without a partial capping layer must have experienced an unintended ripening time due to the remaining heat on the substrate manipulator during the cooling stage, even if no power was delivered to the heater after the InAs QD deposition. It should be mentioned from the AFM images [Figs. 3(b)–3(e)] that the InAs nanostructure heights were increased as the GI time was increased, which explains the PL red-shifts observed in Fig. 2(c). Also, group III intermixing during capping could be considered to explain the PL shifts as it was observed for InAs/GaAs QDs.²⁰ However, because of the high indium content in the InAlGaAs cap, we disregarded group III intermixing as a possible cause for the observed PL red-shift.

D. Transmission electron microscopy

We carried out TEM on a sample with three stacks of InAs QDash layers (GI = 0 s) to confirm the morphology of the buried InAs nanostructures. The LM InAlGaAs spacing layers between the QDash layers are 40 nm thick. We prepared two separate TEM specimens from the sample to examine the morphology of the buried nanostructures under two different $[110]$ and $[1\bar{1}0]$ zone-axis orientations.²⁷ A bright-field two-beam condition $\mathbf{g} = (002)$ was used to increase the chemical-contrast between the InAs nanostructure and InAlGaAs spacing layers.²⁹ In this imaging condition, the InAs QDashes look darker than the LM InAlGaAs spacing layer. The X-TEM images of Fig. 4 clearly reveal that the lateral size of the InAs nanostructure along the $[110]$ direction is smaller than the $[1\bar{1}0]$ direction, which is consistent with the AFM image of Fig. 3(a). The average size of the QDashes is ~ 12 nm along $[110]$, as shown in Fig. 4(a). On the contrary, the cross-sectional TEM image [Fig. 4(b)] projected close to $[110]$ shows that the QDash size along $[1\bar{1}0]$ ranges from ~ 20 to ~ 50 nm. The thin white contrast lines above and below the QDashes are the 3 nm $\text{In}_{0.497}\text{Al}_{0.353}\text{Ga}_{0.15}\text{As}$ cap and 2 MLs of $\text{Al}_{0.5}\text{Ga}_{0.5}\text{As}$ pre-layer, respectively. This TEM investigation undoubtedly proves that the InAs nanostructures without

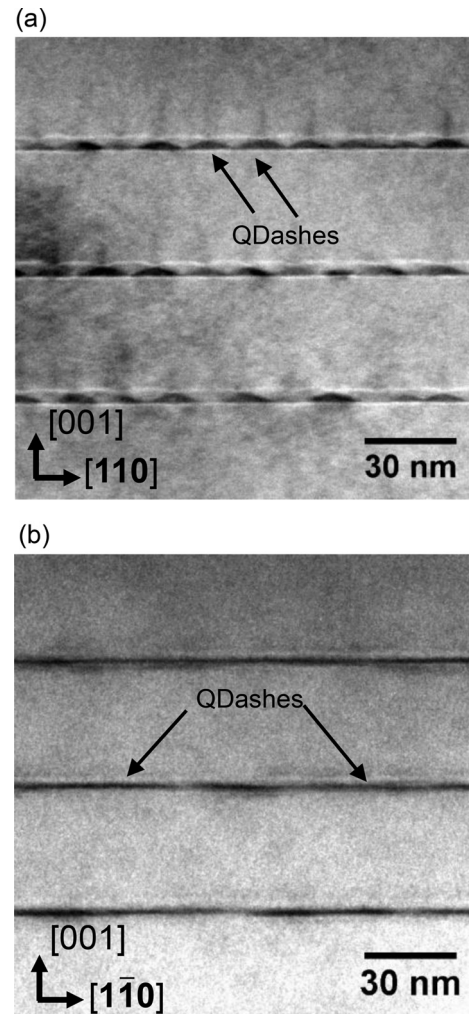


FIG. 4. Cross-sectional TEM images showing three stacks of InAs QDashes with no GI. (a) zone-axis orientation is close to $[1\bar{1}0]$. (b) zone-axis orientation is close to $[110]$. Both images are under $\mathbf{g} = (002)$ two-beam condition.

sufficient GI are first grown in QDashes instead of round-shaped QDs.

IV. CONCLUSION

In conclusion, we have shown that InAs nanostructures grown on InAlGaAs/InP buffers formed in elongated QDashes initially and transformed to round-shaped QDs during the growth interruption. Residual heat on the substrate heater causes unintended ripening of the surface InAs QDs during sample quenching. Partial capping effectively prevented the surface QDs from reforming their shapes during the cooling stage and clearly revealed the evolution of the InAs/InAlGaAs nanostructures. The PL peak wavelength red-shifts from the samples with the growth interruption time from 0 s to 60 s were explained by the increased heights of the InAs nanostructures. The TEM studies confirmed the presence of buried InAs QDashes when the growth interruption was not applied. Therefore, we conclude that improper sample removal can cause an unintended ripening process of surface nanostructures and that surface analysis results in misunderstanding of the morphology of buried quantum dots.

ACKNOWLEDGMENTS

This work was supported by Advanced Research Projects Agency-Energy (ARPA-E, DE-AR0000672). We are also grateful to Kurt Olsson and John English for their assistance in MBE maintenance and Alan Liu and Professor Chris Palmstrøm for fruitful discussions. The work at UT-Austin was supported by NSF NSF-ECCS-1408302 and a Multidisciplinary University Research Initiative from the Air Force Office of Scientific Research (AFOSR MURI Award No. FA9550-12-10488).

- ¹T. Kageyama, K. Takada, K. Nishi, M. Yamaguchi, R. Mochida, Y. Maeda, H. Kondo, K. Takemasa, Y. Tanaka, T. Yamamoto, M. Sugawara, and Y. Arakawa, *Proc. SPIE* **8277**, 72 (2012).
- ²P. G. Eliseev, H. Li, G. T. Liu, A. Stintz, T. C. Newell, L. F. Lester, and K. J. Malloy, *IEEE J. Sel. Top. Quantum Electron.* **7**(2), 135 (2001).
- ³A. Y. Liu, J. Peters, X. Huang, D. Jung, J. Norman, M. L. Lee, A. C. Gossard, and J. E. Bowers, *Opt. Lett.* **42**(2), 338 (2017).
- ⁴J. Brault, M. Gendry, G. Grenet, G. Hollinger, Y. Desieres, and T. Benyattou, *Appl. Phys. Lett.* **73**(20), 2932 (1998).
- ⁵L. Gonzalez, J. M. Garcia, R. Garcia, F. Briones, J. Martinez-Pastor, and C. Ballesteros, *Appl. Phys. Lett.* **76**(9), 1104 (2000).
- ⁶M. Z. M. Khan, T. K. Ng, and B. S. Ooi, *Prog. Quantum Electron.* **38**(6), 237 (2014).
- ⁷J. Brault, M. Gendry, G. Grenet, G. Hollinger, J. Olivares, B. Salem, T. Benyattou, and G. Bremond, *J. Appl. Phys.* **92**(1), 506 (2002).
- ⁸N. Sritirawisarn, F. W. M. van Otten, T. J. Eijkemans, and R. Notzel, *J. Cryst. Growth* **305**(1), 63 (2007).
- ⁹P. Caroff, C. Paranthoen, C. Platz, O. Dehaese, H. Folliot, N. Bertru, C. Labbe, R. Piron, E. Homeyer, A. Le Corre, and S. Loualiche, *Appl. Phys. Lett.* **87**(24), 243107 (2005).
- ¹⁰C. Gilfert, E. M. Pavelescu, and J. P. Reithmaier, *Appl. Phys. Lett.* **96**, 191903 (2010).
- ¹¹J. S. Kim, J. H. Lee, S. U. Hong, W. S. Han, H. S. Kwack, C. W. Lee, and D. K. Oh, *J. Cryst. Growth* **259**(3), 252 (2003).
- ¹²S. Banyoudeh and J. P. Reithmaier, *J. Cryst. Growth* **425**, 299 (2015).
- ¹³N. X. Li, T. Daniels-Race, and M. A. Hasan, *Appl. Phys. Lett.* **80**(8), 1367 (2002).
- ¹⁴A. Stintz, T. J. Rotter, and K. J. Malloy, *J. Cryst. Growth* **255**(3-4), 266 (2003).
- ¹⁵P. J. Poole, J. McCaffrey, R. L. Williams, J. Lefebvre, and D. Chithrani, *J. Vac. Sci. Technol. B* **19**(4), 1467 (2001).
- ¹⁶B. Z. Wang, S. J. Chua, Z. J. Wang, and S. Y. Liu, *Physica E* **8**(3), 290 (2000).
- ¹⁷J. S. Kim, J. H. Lee, S. U. Hong, H. S. Kwack, B. S. Choi, and D. K. Oh, *IEEE Photonics Technol. Lett.* **18**(4), 595 (2006).
- ¹⁸V. I. Sichkovskiy, M. Waniczek, and J. P. Reithmaier, *Appl. Phys. Lett.* **102**(22), 221117 (2013).
- ¹⁹S. Bhowmick, M. Z. Baten, T. Frost, B. S. Ooi, and P. Bhattacharya, *IEEE J. Quantum. Electron* **50**(1), 7 (2014).
- ²⁰J. M. Garcia, G. MedeirosRibeiro, K. Schmidt, T. Ngo, J. L. Feng, A. Lorke, J. Kotthaus, and P. M. Petroff, *Appl. Phys. Lett.* **71**(14), 2014 (1997).
- ²¹S. Barik, H. H. Tan, and C. Jagadish, *Nanotechnology* **17**(8), 1867 (2006).
- ²²B. Shi and K. M. Lau, *J. Cryst. Growth* **433**, 19 (2016).
- ²³J. S. Kim, J. H. Lee, S. U. Hong, W. S. Han, H. S. Kwack, and D. K. Oh, *Appl. Phys. Lett.* **83**(18), 3785 (2003).
- ²⁴C. Paranthoen, N. Bertru, O. Dehaese, A. Le Corre, S. Loualiche, B. Lambert, and G. Patriarche, *Appl. Phys. Lett.* **78**(12), 1751 (2001).
- ²⁵T. J. Krzyzewski and T. S. Jones, *J. Appl. Phys.* **96**(1), 668 (2004).
- ²⁶A. Y. Liu, C. Zhang, A. Snyder, D. Lubyshev, J. M. Fastenau, A. W. K. Liu, A. C. Gossard, and J. E. Bowers, *J. Vac. Sci. Technol. B* **32**(2), 02C108 (2014).
- ²⁷W. Lei, Y. H. Chen, P. Jin, X. L. Ye, Y. L. Wang, B. Xu, and Z. G. Wang, *Appl. Phys. Lett.* **88**, 063114 (2006).
- ²⁸M. Rosini, M. C. Righi, P. Kratzer, and R. Magri, *Phys. Rev. B* **79**(7), 075302 (2009).
- ²⁹K. Cui, M. D. Robertson, B. J. Robinson, C. M. Andrei, D. A. Thompson, and G. A. Botton, *J. Appl. Phys.* **105**(9), 094313 (2009).